

Effect of cholesterol on diffusion in surfactant bilayers

Thorsten Pieper^{a)}*University of Dortmund, Exp. Physics III, Dortmund D-44221, Germany and RIES, Hokkaido University, Sapporo 060-0812, Japan*

Svetlana Markova

University of Dortmund, Exp. Physics III, Dortmund D-44221, Germany

Masataka Kinjo

RIES, Hokkaido University, Sapporo 060-0812, Japan

Dieter Suter

University of Dortmund, Exp. Physics III, Dortmund D-44221, Germany

(Received 19 March 2007; accepted 12 September 2007; published online 29 October 2007)

Biological membranes consist of lipid bilayers with liquid-ordered and liquid-disordered phases. It is believed that cholesterol controls the size of the microdomains in the liquid-ordered phase and thereby affects the mobility as well as the permeability of the membrane. We study this process in a model system consisting of the nonionic surfactant $C_{12}E_5$ and water in the lamellar phase. We measure the diffusion of fluorescent probe molecules (rhodamine B) by fluorescence correlation spectroscopy. For different surfactant to water ratios, we measure how the molecular mobility varies with the amount of cholesterol added. We find that a reduction of the diffusion coefficient is already detectable at a molar ratio of 8 mol % cholesterol. © 2007 American Institute of Physics. [DOI: 10.1063/1.2794345]

I. INTRODUCTION

In eukaryotic cells, the plasma membrane is mainly composed of glycerophospholipids, sphingolipids, and a sterol. The amphiphilic structure of the lipid molecules results in the formation of a bilayer membrane. For their function, cells need an exchange of molecules and ions with their surrounding through the cell membrane. The knowledge of how these transport processes are controlled by the cell is important, e.g., for the development of pharmaceuticals. The fact that the composition of the cell membrane is maintained by intracellular functions suggests that it is a key factor for the cell's life cycle and communication. Especially the cholesterol and lipid contents of the membrane play an important role for the regulation of protein transport inside and outside the cell.¹ Cholesterol within the membrane has an influence on the molecular order by hydrophobic and steric interactions.^{2,3}

Mechanical properties of cell membranes as well as the exchange of matter through the membranes depend strongly on the diffusion of lipid molecules inside the membrane. To study diffusion in membranes, several methods have been used. Light scattering and NMR methods provide high precision due to averaging over large ensembles of particles. On the other hand, when diffusion on small scales with a few or even single molecules is observed, fluorescence microscopy methods provide a better way to determine more interesting properties. For this study, fluorescence correlation spectroscopy

(FCS) was chosen as an experimental technique offering the advantages of small sample volumes and short measurement times.

Because of the similarity between the lamellar phase of surfactant/water emulsions and the biological cell membrane, they have been considered as simplified model systems for membranes. Microemulsions of surfactants and water can show a variety of structures. The transitions between the different phases depend on the composition and on external parameters such as temperature and pressure. Adding other substances to the system can also affect the phase transitions and the properties of the individual phases. In this paper, we study the effect of cholesterol on the surfactant/water system, in particular, the lamellar phase.

By using a surfactant/water model, the fundamental influence of cholesterol incorporated in bilayers is examined. In contrast to lipids of biological membranes, the chosen surfactant consists of a headgroup and a single saturated dodecyl chain. The molecular order of the system is simplified compared to biological membranes composed of a variety of complex lipids. It is shown that cholesterol does not reduce diffusional mobility in complex structures only but in basic lipid assemblies as well.

The paper is structured as follows. In Sec. II the chemical system and its components are described. Section III briefly explains fluorescence correlation spectroscopy as the experimental method. The correlation functions for the analysis of the measurements are introduced and the calibration procedure is discussed. In Sec. IV, the experiments and the results are summarized. An interpretation and comparison with the existing literature are given in Sec. V.

^{a)}Electronic mail: thorsten.pieper@gmx.de

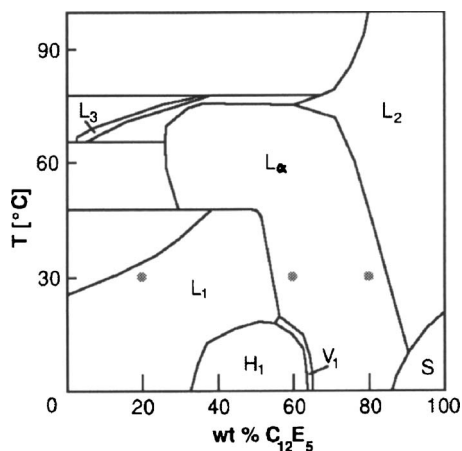


FIG. 1. Phase diagram of $C_{12}E_5$ and H_2O . L_1 and L_α denote the micellar and the lamellar phase, respectively. H_1 is the hexagonal phase, and L_2 and S the inverse micellar and the solid phase. V_1 is the cubic phase. L_3 is a sponge phase. Unnamed areas are bicontinuous. The component ratios that were measured are marked with gray dots. The image was redrawn from Mitchell *et al.* (Ref. 27).

II. MEMBRANE SYSTEM

A. Components

$C_{12}E_5$. For the model membrane, we chose the system $C_{12}E_5$ /water. The nonionic surfactant pentaethylene glycol monododecyl ether ($C_{12}E_5$) was obtained from SigmaAldrich (St. Louis, MO). For the molecule length values from 22 to 26 Å were reported.^{4,5} The critical micelle concentration is 64 μM at 25 °C.⁶ As can be seen in the phase diagram (Fig. 1), the emulsion of $C_{12}E_5$ and H_2O shows different molecular orders depending on the surfactant concentration and temperature.

R18. A fluorescent marker molecule is required to detect light from the transparent specimen. For this purpose, we chose octadecyl rhodamine B, R18 ($D=420 \mu\text{m}^2/\text{s}$ in water, $M=731.5 \text{ g mol}^{-1}$). The excitation and emission maxima are 555 and 578 nm, respectively. R18 is an amphiphilic molecule with a polar head and an unpolar tail. We expect that the dye molecules enter into the lipid phase and probe its mobility. There is no information available if R18 prefers the liquid-ordered or liquid-disordered phase.

Cholesterol. Cholesterol has a molecular weight of 386.65 g mol^{-1} . The molecule length is 16 Å. The chemical structures of R18 and cholesterol are depicted in Fig. 2.

B. Preparation of surfactant emulsions

Lipid and cholesterol were weighed with a microbalance, vortexed, heated, and sonicated until the system became completely homogeneous. Then milliQ water containing fluorescent dye was added. The 20 wt % $C_{12}E_5$ and the 60% solutions contained $10^{-8}M$ R18, while the concentration in the 80% solution was $10^{-7}M$. The samples were then again heated to 60–70 °C, sonicated, vortexed, and frozen (–80 °C). These steps were repeated until the samples had become homogeneous gels. For the nominal 60 wt % emulsions, the fraction of $C_{12}E_5$ and cholesterol varied between 0.596 and 0.643. In the subsequent measurements of the

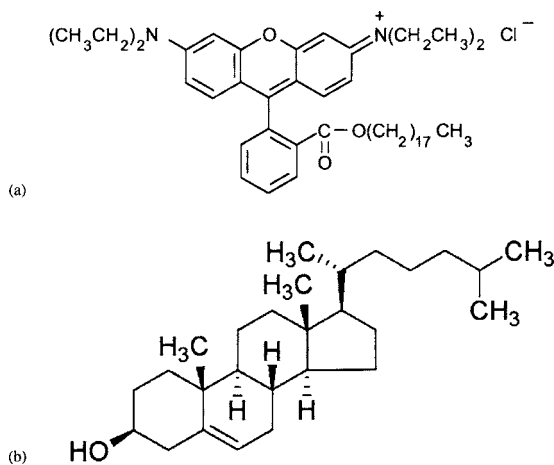


FIG. 2. Structures of (a) R18 and (b) cholesterol.

80 wt % emulsion, the lipid fraction was kept constant at 0.80. The ratios of substances are listed in Table I.

C. Micellar phase

In the micellar phase, the dye molecules enter the micelle and the observed diffusion will be that of the micelle. From standard diffusion theory, we expect that the diffusion coefficient D is related to the size of the micelles by

$$D = \frac{k_B T \ln(2r)}{6\pi\eta a}. \quad (1)$$

η is the viscosity of the solvent, k_B the Boltzmann constant, and T the Kelvin temperature. We will assume that the mi-

TABLE I. The table subsumes the amount of substances used in the micro-emulsions. The ratio value gives the molar ratio of cholesterol vs $C_{12}E_5$. The lipid frac. value denotes the fraction of $C_{12}E_5$ and cholesterol.

Phase (wt %)	$C_{12}E_5$ (mg)	Chol. (mg)	H_2O (mg)	Ratio	Lipid frac.
Mic 20	80	0	320	0	0.20
Lam 60	243.5	48.8	162.6	0.211	0.643
	233.7	38.1	154.8	0.171	0.637
	255.3	38.3	170.7	0.158	0.632
	230.5	33.9	156.8	0.155	0.628
	243.2	31.3	163.0	0.135	0.627
	267.7	31.5	177.7	0.124	0.627
	255.6	25.3	168.9	0.104	0.624
	199.3	19.6	132.9	0.103	0.622
	250.0	21.4	167.5	0.090	0.618
	227.1	16.8	151.6	0.078	0.617
	219.7	12.1	145.8	0.058	0.614
	253.6	9.7	173.6	0.040	0.603
	229.4	8.2	153.6	0.038	0.607
227.0	4.1	156.8	0.019	0.596	
Lam 80	153.8	3.05	40.7	0.021	0.794
	159.5	10.75	43.4	0.071	0.797
	159.0	15.7	44.6	0.104	0.797
	159.4	17.2	44.4	0.113	0.799
	155.8	20.5	45.0	0.138	0.797
	159.5	26.8	48.2	0.177	0.794

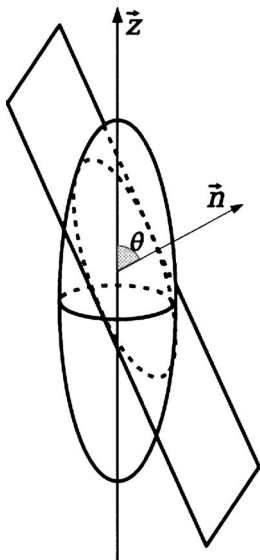


FIG. 3. Sketch of the orientation model: In the lamellar phase, molecular diffusion is thought to be restricted to two-dimensional planes intersecting the focus intensity distribution at arbitrary angles θ and vertical intercepts. Integrating the contributions from different orientations results in an effective angle $\theta = \theta_m$.

cells are prolate ellipsoids with a long axis a and an axis ratio $r \gg 1$.

D. Lamellar phase

In the lamellar phase, the lipid molecules form a bilayer structure. The membrane layer thickness is about double the length of a surfactant molecule $\delta = 2l_s$. The repeat distance of the lamellar structure is

$$X_{\text{lam}} = 2l_s / \phi_s, \quad (2)$$

where ϕ_s is the volume fraction of the surfactant in the emulsion. Assuming $\phi_s = 0.6$ (0.8) and $l_s = 26 \text{ \AA}$, the repeat distance has a value of $X_{\text{lam}} = 8.7 \text{ nm}$ (6.5 nm).

The molecular order of the lamellar phase is maintained by van der Waals forces between the alkyl chains and hydrogen bonding forces between water molecules and the lipid headgroups.⁷

During the FCS measurements, we probe the bilayer dynamics in a volume of $\approx 0.5 \mu\text{m}^3$, at a distance of $60 \mu\text{m}$ from the cover glass surface. Because this distance leaves room for about 7000–9000 bilayers, we may assume that surface effects are no longer important and the bilayers are randomly oriented. Additionally, we varied the horizontal alignment of the measurement position to different positions across the sample drop. We expect that the remaining orientations of bilayers are averaged out by repeated measurements.

The molecular diffusion of each molecule is restricted to a single two-dimensional bilayer. The resulting propagation differs from that of free diffusion,⁸ but the observed signal represents an average over all possible orientations (see Fig. 3). Within the laser focus, which represents the sensitive volume, there is room for about 50 bilayers when they are arranged horizontally and 300 when they are arranged vertically.

Following the procedure of Galla and Sackmann for proteins and lipids in biological membranes,⁹ we relate the diffusion of dye and lipid molecules to their molecular weights as

$$D_{\text{dye}} = D_{\text{lipid}} \left(\frac{M_{\text{lipid}}}{M_{\text{dye}}} \right)^{1/2}. \quad (3)$$

When $C_{12}E_5$ is compared to R18, the correction factor is 0.75.

Experimental data show that the shear viscosity in such binary or ternary systems can easily span orders of magnitude from 1 mPa s to 10^5 Pa s, depending on concentration, pressure, and temperature,^{10–12} but the effect of cholesterol on these parameters has not been studied so far.

III. FCS MEASUREMENTS

FCS is a method basically used to determine low concentrations and diffusion coefficients in liquid environments. The sensitivity in FCS is on the single molecule level and the measurements are direct results from the observation of a small ensemble of molecules. Ensemble averaging is necessary for the standard correlation function approach that was proposed by Magde and Elson in 1974.^{13,14}

The key in FCS is the reduction of the observation volume by using a confocal microscope. The confocal principle is a simple way to collocate the excitation and observation volume of a strongly focused light spot. In the focus center, fluorescent molecules emit photons shifted to longer wavelengths in response to electronic excitation. This light is separated from the excitation light by an optical filter. Background light is suppressed by an aperture placed in the back focal plane. The fluorescence time series $I(t)$ is detected with a photodiode and from $I(t)$ the autocorrelation is computed in correlator hardware. The correlation curve contains the temporal information about processes that affect the fluctuating signal in a nonstochastic manner,

$$G(\tau) = 1 + \frac{\langle \delta I(t) \delta I(t + \tau) \rangle}{\langle I \rangle^2}, \quad \delta I(t) = I(t) - \langle I \rangle. \quad (4)$$

$\langle \dots \rangle$ denotes the time average. In the limit $\tau \rightarrow 0$, $G(\tau) - 1$ is inversely proportional to the average number N of fluorescing molecules in the observation volume. We assume that diffusion is the dominant process that causes the change in the intensity and call the time where $G(\tau) - 1$ has decreased to $0.5N^{-1}\sqrt{1+K^{-2}}$ the diffusion time average τ_d . $K = z_0/w_0$ denotes the ratio between the length and width of the focus, which is known as the structure parameter. From the diffusion time, we calculate the diffusion coefficient D as

$$D = \frac{w_0^2}{4\tau_d}. \quad (5)$$

After calibrating the focus parameter w_0 with a known standard, the diffusion coefficient of other molecules can be determined.

The spatial resolution of FCS lies within the range of the optical diffraction limit of the excitation wavelength. The temporal resolution depends on the dead time of the photon

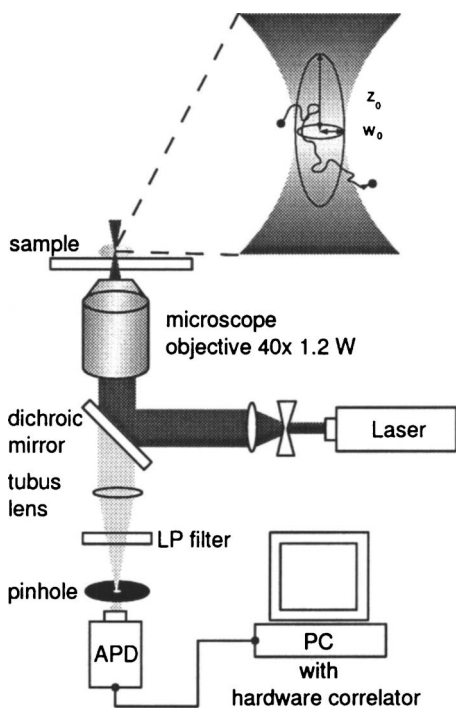


FIG. 4. Confocal microscope setup for FCS and schematic of the observation volume with half-axes w_0 and z_0 (enlarged).

detector and the sampling time of the correlator, which is 200 ns here. The diffusion time/molecule is typically between 0.2 and 3 ms.

A. Setup

Our setup uses a Zeiss ConfoCor 2 (Oberkochen, Germany) inverted microscope with a motorized stage. The objective is a Zeiss C-Apochromat 40 \times with a numerical aperture of 1.2, water immersion type. It is equipped with a correction ring for varying cover glass thicknesses. A constant temperature in the sample chamber is maintained by an electronically controlled holder. The HeNe laser [LGK 7786 P from Lasos (Jena, Germany)] works at a wavelength of 543 nm. The laser power is reduced to 100 μ W by an acousto-optic tunable filter. The detection channel consists of a variable pinhole, which is set to a diameter of 78 μ m. The fluorescence signal is detected by a built-in photodiode, SPCM-AQR 13, from Perkin-Elmer (Wellesley, MA). The emission light passes a long pass emission filter with a cutoff wavelength of 560 nm. A schematic picture of the setup is drawn in Fig. 4.

B. Calibration

The focus parameters were calibrated with a 10^{-8} M aqueous solution of rhodamine 6G. The waist parameter determined in this way fell between $w_0=0.22$ and 0.25 μ m, with an average of $\bar{w}_0=0.241$ μ m. The structure parameter K was set to a fixed value of 6.0 corresponding to a vertical focus radius of $z_0=1.3$ – 1.5 μ m. A theoretical calculation using the formula of Rigler *et al.*¹⁵ results in a slightly smaller value for w_{th} ,

$$w_{th} \geq \frac{\lambda_{exc}}{n\pi \tan(\alpha/2)} = 0.206 \mu\text{m}, \quad (6)$$

$$z_{th} \approx \frac{es_0}{\tan \alpha} 0.72 = 1.8 \mu\text{m}.$$

Here, n is the refractive index of the sample which equals the one for pure water, 1.33. The values hold under ideal conditions of a Gaussian beam profile and an optimal aperture position. The finite size of the objective's illuminated rear side puts an upper limit on the focusing half-angle $\alpha = \arcsin(NA/n)$. s_0 is the pinhole radius divided by the magnification. z_{th} must be corrected by a factor of 0.72 depending on the value of $\sin \alpha$ (0.84–0.9 here).

Adding $C_{12}E_5$ to pure water changes the refractive index of the sample solution. Hamano *et al.* gave a linear equation to calculate the refractive index of a $C_{12}E_5$ /water mixture¹⁶ for a wavelength of 633 nm and a temperature of 20 $^\circ$ C. According to this, the mixtures consisting of 20, 60, and 80 wt % $C_{12}E_5$ have refractive indices of $n'=1.357$, 1.407, and 1.432.

The difference in optical refraction changes the size of the focused laser spot. Taking this into account, we estimate the focus waist in these three media to be $\hat{w}_0=0.247$, 0.256, and 0.261, respectively. These values were used in the evaluation of the correlation functions.

Two additional experimental adjustments were done to take the different refractive indices into account. The microscope objective has a correction ring which can be used to adjust the refraction properties to varying cover glass thicknesses. Measurement series with 20 and 50 wt % $C_{12}E_5$ emulsions showed the highest fluorescence count rates if the correction ring is in the maximum position of 0.18 μ m. In all following experiments the correction ring was kept in this position. Secondly, the length of the optical light path was reduced by setting the focus to a position 60 ± 1 μ m above the cover glass surface.

C. Autocorrelation model functions

The standard model function $G(\tau)$ for one fluorescent species diffusing freely in three dimensions and a Gaussian detection volume¹⁷ is given by

$$G(\tau) = 1 + \frac{1}{N} \left(1 + \frac{p_t}{1-p_t} e^{-\tau/\tau_t} \right) \left(1 + \frac{\tau}{\tau_d} \right)^{-1} \left(1 + \frac{\tau}{K^2 \tau_d} \right)^{-0.5}. \quad (7)$$

Here, N is the average number of molecules in the detection volume $V_0 = \pi^{3/2} w_0^2 z_0$. p_t and τ_t represent the triplet fraction and time. The contribution from the triplet dark state is small as long as the laser intensity is low.

As we will discuss in the following section, this standard model proved to be unsatisfactory for the analysis of the diffusion measurements in the lamellar phase. We relate this to the fact that the molecules are not free to diffuse in three dimensions, but are confined to the two-dimensional bilayers. The orientation of these bilayers with respect to the laser

beam is random, so the measurements detect an orientational average. We found that the following equation can be used to describe the experimental correlation data:

$$G_o(\tau) = 1 + \frac{1}{N} \left(1 + \frac{p_t}{1-p_t} e^{-\tau/\tau_t} \right) \left(1 + \frac{\tau}{\tau_d} \right)^{-0.5(1+\cos\theta_m)} \times \left(1 + \frac{\tau}{K^2\tau_d} \right)^{-0.5\sin\theta_m} \quad (8)$$

θ_m is equal to the magic angle $\theta_m = \arccos(1/\sqrt{3}) \approx 54.7^\circ$. We will refer to this model as the orientation model. It is based on a single diffusion coefficient. Compared to the standard model with the same diffusion coefficient, Eq. (8) shifts the function to a longer apparent diffusion time. A detailed analysis of this model will be published later.

The counts/molecule value $\text{cpm} = \text{CR}/N$ is the fraction of the fluorescent count rate CR and the number of molecules in the detection volume. It depends on the dye properties, the solvent, quenching effects, scattering processes, and the detection system (alignment, filters, efficiencies).

IV. EXPERIMENTS

A. Procedure

During the FCS experiments, the samples were placed in Lab-Tek 8-NUNC sample chambers. The bottom glass type is borosilicate 1 with a thickness from 0.13 to 0.16 μm . The micellar emulsions are liquid and four to five drops can be poured into the chambers. For the highly viscous gel emulsions (60% surfactant and more) a spatula must be used. The vessel was placed into the holder and covered with a non-transparent lid. The temperature control unit was set to 30 $^\circ\text{C}$. Table I lists the different samples that were used for this study, showing the different molar ratios of cholesterol and C_{12}E_5 .

Five subsequent correlation functions of 30 s each were averaged for one measurement. For each sample, we performed 8–20 measurement runs. The correlation functions were fitted to the theoretical expressions of Eq. (7), Eq. (8) to determine the diffusion time and, using Eq. (5), the diffusion coefficients. Additionally, the cpm value was determined.

B. Results

Figure 5 shows a typical measurement result from the micellar phase for a sample of 20 wt % C_{12}E_5 . The experimental correlation data were fitted with the standard model for free diffusion, Eq. (7). The best fit was obtained for the average parameters $\tau_d = 2.8 \pm 0.8$ ms, $N = 0.32 \pm 0.03$, $\tau_t = 3$ μs , and $p_t = 0.14$. According to Eq. (5), this corresponds to a diffusion coefficient $D_{\text{mic}} = 5.4 \pm 2$ $\mu\text{m}^2/\text{s}$. This value agrees with the expectation that it arises from the diffusion of prolate micelles. Their average size can be estimated using Eq. (1) presuming an axis ratio of 40:1.¹⁸ We obtain a result of $a = 180$ nm for the long axis. For the given sample, this amounts to about 5000 micelles in the focus volume, of which on average $N = 0.32 \pm 0.03$ carry a fluorescent molecule.

In the lamellar phase two different ratios of C_{12}E_5 and water were examined, 60 and 80 wt % surfactants. In this

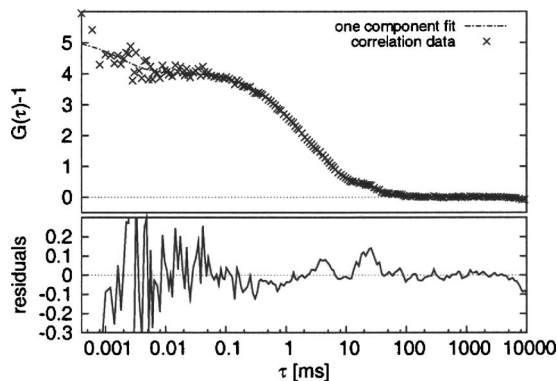


FIG. 5. FCS data for the micellar phase. The diffusion time in this example is $\tau_d = 1.99 \pm 0.05$ ms.

case, fluorophores diffuse independently within the lipid bilayers. The average number of molecules in the detection volume is 1.1 ± 0.3 for the low concentrated lamellar and 11 ± 6 for the high concentrated lamellar phase. The higher value for the 80% lamellar phase was expected from the sample preparation.

When we fitted these data with the standard model of unrestricted (three-dimensional) diffusion [Eq. (7)], we found a significant deviation, as shown in Fig. 6. However, we find no systematic deviation if we fit the experimental data to the orientation model, Eq. (8). For the example shown in Fig. 6, the two models yield diffusion times of $\tau_d = 1.32 \pm 0.02$ ms (standard model) and $\tau_d = 0.901 \pm 0.008$ ms (orientation model), corresponding to diffusion constants D of 12.4 and 18.2 $\mu\text{m}^2/\text{s}$. While this analysis results in different values for the diffusion constants, the dependence on the cholesterol content did not change. The values of the measured diffusion constants were consistent with the assumption that the fluorescent R18 molecules were confined to the lipid bilayers. To check for a fraction of R18 in the water phase, we also fitted the data to a two-component model function. The results showed no significant component with a high diffusion constant.

Figure 7 summarizes the change of the diffusion constant in the 60% lamellar phase upon the addition of chole-

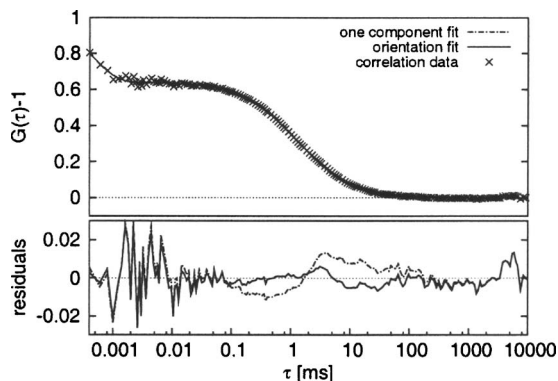


FIG. 6. Example for the FCS data from the surfactant/cholesterol/water emulsion. The experimental data (crosses) are compared to best fits using the standard (single-component) model (dashed-dotted line) and to the orientation model (full line). The cholesterol to surfactant ratio was 0.172. The diffusion times are $\tau_d = 1.32 \pm 0.02$ ms (standard model) and $\tau_d = 0.901 \pm 0.008$ ms (orientation model).

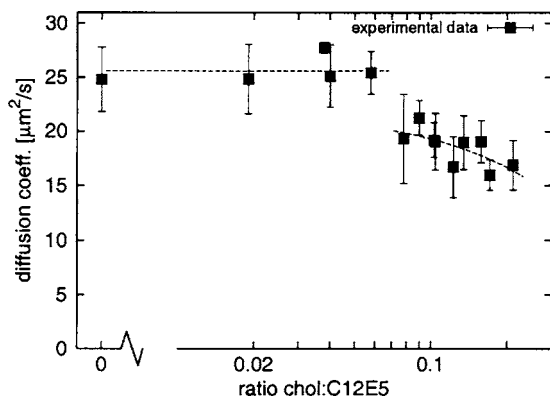


FIG. 7. Result for the diffusion coefficient D of R18 in the lamellar phase with 60 wt % surfactant. The molar ratio of cholesterol to surfactant increases to the right. A reduction in molecular mobility is apparent at a ratio of 0.08. Error bars denote the standard deviation. Guidelines for the eyes are drawn as dashed lines.

terol. At low concentrations, no substantial effect is visible, but at a cholesterol content of about 8%, a sudden reduction by $\approx 20\%$ occurs. A further increase of the cholesterol concentration yields an additional continuous reduction. The total decrease in the molecular mobility is $\approx 30\%$ for a cholesterol molar ratio of 0.2.

The same measurements were also performed for the samples with the higher lipid contents. As shown in Fig. 8, the diffusion constant for low cholesterol content is approximately half of the corresponding data for the 60% system. Again, a sudden decrease of the mobility is observed at a cholesterol content of $\approx 8\%$ and a continuous decrease at higher concentrations.

The triplet fraction in the correlation amplitude is at 16% on the average. The cpm value is between 11 and 14 kHz for low concentrations of cholesterol. Increasing the cholesterol concentration reduces the count rate by up to 50% (Fig. 9). This may be a consequence of increased scattering in these samples. Visually observable was a small turbidity in the sample with a cholesterol ratio of 0.2 at room temperature. Alternatively, the effect may be due to fluorescence quenching by cholesterol.

In addition to the graphical representation of the diffusion data, Table II also gives the numerical values for the extreme cases. The last column of this table also shows the

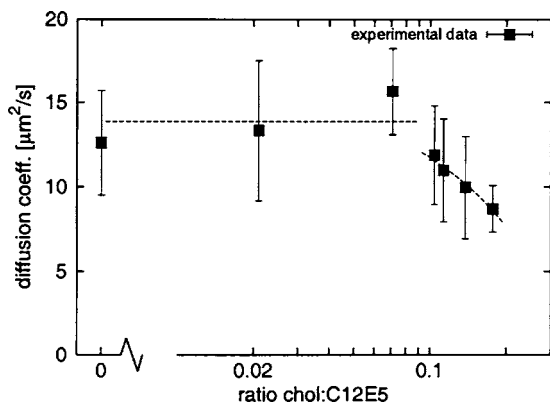


FIG. 8. Diffusion coefficients for the 80 wt % surfactant emulsion as a function of the cholesterol content.

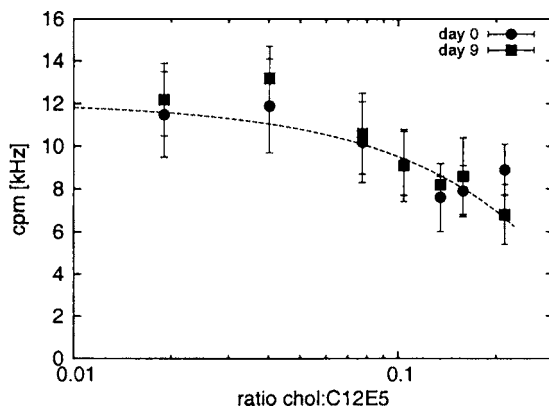


FIG. 9. Counts/molecule value (cpm) as a function of cholesterol content from the same sample on two different days. The brightness is reduced by increasing cholesterol content.

inferred diffusion constants of the lipid molecules, which were calculated from the measured diffusion constants by correcting for the different molecular weights using Eq. (3).

V. DISCUSSION AND CONCLUSION

We have measured the diffusion of fluorescent probe molecules in the $C_{12}E_5$ /water system. In the micellar phase (at 20 wt % lipid concentration), the observed correlation function is consistent with a model of freely diffusing micelles with a length of the order of 180 nm and a given axis ratio of 40:1. This size might be an overestimate, since the interaction between the micelles should result in a small diffusion constant than for micelles at low concentrations. Using this value, an upper limit of 0.14 as the total volume fraction of micelles in the solution can be given. Here, the volume reduction of the micellar solution of about 7% was already taken into account.

The lamellar system does not show free, three-dimensional diffusion. The correlation curves rather suggest that the Brownian motion of the probe molecules is restricted to the lamellar bilayers. The orientation model that we used for the analysis of the correlation function takes into account an average over many bilayer orientations and yields plausible fitting results.

The measured diffusion coefficients are generally higher than in dimyristoyl phosphatidylcholine (DMPC) membranes at equal temperature.¹⁹ This is attributed to the higher rigidity of DMPC membranes. Regarding the influence of cholesterol, we can conclude that a cholesterol addition above a fraction of 0.08 in the $C_{12}E_5$ bilayer reduces the molecular

TABLE II. Overview of diffusion coefficients D in $C_{12}E_5$ /water/cholesterol emulsions determined from the orientation model.

$C_{12}E_5$ (wt %)	Phase	chol: $C_{12}E_5$ ratio	D (probe) ($\mu\text{m}^2/\text{s}$)	D (lipid) ($\mu\text{m}^2/\text{s}$)
20	Micellar	...	5.4	...
60	Lamellar	0	26	34
60	Lamellar	≈ 0.2	16	21
80	Lamellar	0	14	19
80	Lamellar	≈ 0.2	9	12

mobility in the chosen surfactant/water emulsion. Because of the small observation volume in FCS, it is justified to claim that the structural changes of the molecular order take place on a scale below the focus diameter of $0.5\ \mu\text{m}$. This reduction is a consequence of stronger molecular interaction induced by the presence of cholesterol molecules. Comparing this effect with observations in dilauroyl phosphatidylcholine (DLPC), the reduction of D by 30% is slightly smaller than in DLPC where reductions by $\approx 50\%$ were observed at the same cholesterol fraction.²⁰ The reason might be a tighter packing of cholesterol molecules in double chain amphiphiles.

It is known that cholesterol interacts with alkyl chains. There are reports that cholesterol increases the fluidity in the center of DMPC membranes while decreasing it near the polar head group region.²¹ A dependency on the length and asymmetry of the alkyl chains was also found.²² In the present case, cholesterol has about $2/3$ the length of a C_{12}E_5 molecule. Its rigid steroid ring is thought to restrain the free rotational motion of about five to six segments of the surrounding lipid molecules. Compared to biomembranes with lipids being asymmetric and longer, cholesterol may be incorporated differently. Nevertheless, our measurements show a similar influence of cholesterol on diffusion. Apparently, the fluorescent probes do not detect a higher fluidity of the inner alkyl groups, but rather the reduced mobility at the polar/unpolar interface. Here, it is generally assumed that their diffusion is related to the lipid molecules, but an independent verification would certainly be appropriate.

Regarding earlier measurements, it is striking that in the majority of experimental studies, cholesterol was found to decrease the diffusion coefficient in phosphatidylcholine membranes. Molecular dynamics simulations support these findings. Thus, its effect on the molecular order of membranes seems to be a rather universal feature.

There are other effects in artificial membranes that possibly play a role in the correct description of molecular motion. It was reported that molecules diffusing in nanostructured liquids show effects of anomalous diffusion.^{23–25} This can appear, for example, in the presence of coexisting gel and fluid phases. It can also be found in binary solutions of DMPC/distearoyl phosphatidylcholine (DSPC), as recent studies using computer simulations and FCS experiments have indicated.²⁶

In conclusion, our results show a reduction of molecular mobility in a simple surfactant/water system induced by cho-

lesterol at concentrations above 8%. The structural influence of cholesterol seems to be independent of a possible phase transition though it might induce one in higher concentration. Our data help generalize the understanding of chemical interaction between cholesterol and lipids, and thus the principle of the membrane order.

ACKNOWLEDGMENTS

We thank Goro Nishimura and Yu Ohsugi from the Hokkaido University for their help and advice. This project was supported by Grant No. PE05567 from the Japan Society for the Promotion of Science.

- ¹G. W. Feigenson and J. T. Buboltz, *Biophys. J.* **80**, 2775 (2001).
- ²M. Tarshish, M. Salman, and S. Rottem, *Biophys. J.* **64**, 709 (1993).
- ³S. Raffy and J. Teissie, *Biophys. J.* **76**, 2072 (2004).
- ⁴E. Z. Radlinska, T. Gulik-Krzywicki, F. Lafuma, D. Langevin, W. Urbach, C. E. Williams, and R. Ober, *J. Phys. II* **7**, 1393 (1997).
- ⁵S. K. Ghosh, S. Komura, J. Matsuba, H. Seto, T. Takeda, and M. Hikosaka, *Prog. Colloid Polym. Sci.* **106**, 91 (1997).
- ⁶P. D. T. Huibers, V. S. Lobanov, A. R. Katritzky, D. O. Shah, and M. Karelson, *Langmuir* **12**, 1462 (1996).
- ⁷C. Stubenrauch, S. Burauer, R. Strey, and C. Schmidt, *Liq. Cryst.* **31**, 39 (2004).
- ⁸J. Crank, *The Mathematics of Diffusion*, 2nd ed. (Oxford University Press, New York, 1975).
- ⁹H. J. Galla, W. Hartmann, U. Theilen, and E. Sackmann, *J. Membr. Biol.* **48**, 215 (1979).
- ¹⁰S. Paasch, F. Schambil, and M. J. Schwuger, *Langmuir* **5**, 1344 (1989).
- ¹¹G. D'Arrigo and G. Briganti, *Phys. Rev. E* **58**, 713 (1998).
- ¹²J. Schulte, S. Enders, and K. Quitzsch, *Colloid Polym. Sci.* **277**, 827 (1999).
- ¹³E. L. Elson, *Biopolymers* **13**, 1 (1974).
- ¹⁴D. Magde and E. L. Elson, *Biopolymers* **13**, 29 (1974).
- ¹⁵R. Rigler, U. Mets, J. Widengren, and P. Kask, *Eur. Biophys. J.* **22**, 169 (1993).
- ¹⁶K. Hamano, N. Kuwahara, T. Koyama, and S. Harada, *Phys. Rev. A* **32**, 3168 (1985).
- ¹⁷P. Kask, R. Günther, and P. Axhausen, *Eur. Biophys. J.* **25**, 163 (1997).
- ¹⁸M. Jonströmer, B. Jönsson, and B. Lindman, *J. Phys.: Condens. Matter* **95**, 3293 (1991).
- ¹⁹G. Orädd, G. Lindblom, and P. W. Westerman, *Biophys. J.* **83**, 2702 (2002).
- ²⁰J. Korlach, P. Schwille, W. W. Webb, and G. W. Feigenson, *Proc. Natl. Acad. Sci. U.S.A.* **96**, 8461 (1999).
- ²¹J.-J. Yin and W. K. Subczynski, *Biophys. J.* **71**, 832 (1996).
- ²²L. Chena, M. L. Johnson, and R. L. Biltonen, *Biophys. J.* **80**, 254 (2001).
- ²³G. J. Schütz, H. Schindler, and Th. Schmidt, *Biophys. J.* **73**, 1073 (1997).
- ²⁴P. Schwille, J. Korlach, and W. W. Webb, *Cytometry* **36**, 176 (1999).
- ²⁵A. Gennerich and D. Schild, *Biophys. J.* **83**, 510 (2002).
- ²⁶A. E. Hac, H. M. Seeger, M. Fidorra, and T. Heimburg, *Biophys. J.* **88**, 317 (2005).
- ²⁷D. J. Mitchell, G. J. T. Tiddy, L. Waring, T. Bostock, and M. P. McDonald, *J. Chem. Soc., Faraday Trans. 1* **79**, 975 (1983).